ARMA 20–1215

Numerical Modeling of Pillar Stress Redistribution During the Retreat Mining Process

Dean-Pelikan, R. A.
Colorado School of Mines, Golden, CO, USA
Walton, G.
Colorado School of Mines, Golden, CO, USA

This paper was prepared for presentation at the 54th US Rock Mechanics/Geomechanics Symposium held in Golden, Colorado, USA, 28 June-1 July 2020. This paper was selected for presentation at the symposium by an ARMA Technical Program Committee based on a technical and critical review of the paper by a minimum of two technical reviewers. The material, as presented, does not necessarily reflect any position of ARMA, its officers, or members. Electronic reproduction, distribution, or storage of any part of this paper for commercial purposes without the written consent of ARMA is prohibited. Permission to reproduce in print is restricted to an abstract of not more than 200 words; illustrations may not be copied. The abstract must contain conspicuous acknowledgement of where and by whom the paper was presented.

ABSTRACT: Retreat mining creates unstable ground conditions that increase stresses on remaining un-mined pillars. These increasing stresses can in turn lead to unsafe mine conditions. Current understanding of pillar stresses is primarily based on tributary area theory (TAT) and simplified numerical models. To better understand a pillar's strength and stress load during retreat mining, a finite difference software (FLAC3D) was used to model a coal room and pillar mine. The numerical approach can be used to model the actual geometry of retreat mining operations. Also, more complex geomechanical behaviors can be modeled. Variable width to height ratios, material properties, and mining methods/sequences were tested. Of particular interest is how the consideration of inelastic pillar material behavior leads to differences in stress concentration trends from those predicted using a conventional elastic approach. Ultimately, this understanding of how stresses re-distribute during the retreat mining process can help improve the safety of the mining method.

1. INTRODUCTION

A room and pillar coal mine was modeled in order to determine the stress redistribution on pillars during the retreat mining process. Tributary Area Theory (TAT) and simple (elastic) numerical models are conventional methods to determine pillar stresses. These approaches have limitations that tend to lead to conservative results. These results may cause an overestimation of the pillar strength in back analysis of failed cases, which can lead to overconfidence in a pillar's ability to support the overburden (Frith and Reed, 2017). As a result, unsafe mining conditions may be created.

To better understand stresses on pillars during retreat mining, a coal room and pillar mine was modeled using a finite difference software, FLAC3D. Using FLAC3D, the actual geometry of retreat mining operations and more complex geomechanical behaviors can be modeled. Variable width to height ratios, material properties, and mining sequences were modeled to understand how the various parameters impact the stress concentrations on the pillars. Of greatest interest is modeling inelastic behavior to evaluate the differences in stress concentration trends from those predicted by conventional elastic models.

2. RETREAT MINING PROCESS

Retreat mining is a process that is used to mine out pillars that provide stability in the typical room and pillar mining method. The National Institutes for Occupational Safety and Health (NIOSH) found that about 60% of retreat mines use the Christmas tree method and about 35% use the Outside Lift method (NIOSH, 2010). These two methods make up the two most common retreat methods used in coal retreat mines.

Retreat mines often have bleeder entries and barrier pillars in place to maintain some stability. Pillars are then removed in a particular panel, from the bleeder entry towards the mine shaft or entrance. Figure 1 shows a typical layout of a retreat room and pillar mine (Mark, 2009).

2.1. Model Layout and Sequencing

The pillar panel considered in this study follows a 6 x 10 grid pattern. The pillar length and width are dependent on the pillar width to height ratio (W/H), which was varied as part of this study (3 and 6). The pillar height is 3 m. Figure 2 and 3 shows the pillar naming convention as well as the difference in pillar size between the W/H

cases of 3 and 6. The pillars in the x direction are labeled i1 through i6. The pillars in the y direction are labeled j1 through j10.

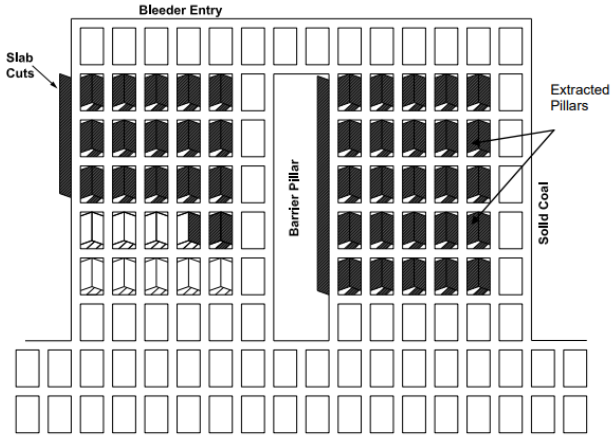

Fig. 1. General layout of a retreat room and pillar mine (NIOSH 2010).

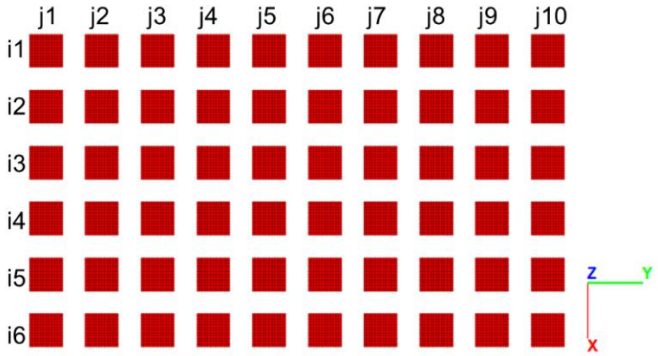

Fig. 2. Pillar naming convention for W/H = 3 case.

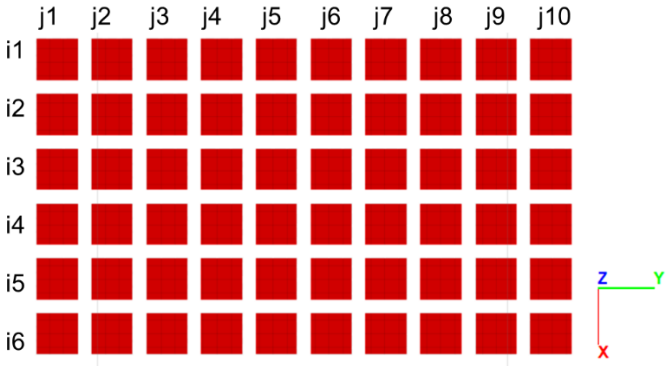

Fig. 3. Pillar naming convention for W/H = 6 case.

Pillars in row i6 and column j1 were not removed, as these pillars are part of the bleeder entry. Accordingly, the panel of pillars to be removed matches the typical layout of a retreat room and pillar mine as shown in Figure 1.

In this study, two similar mining sequences are considered: two pillars extracted simultaneously and a single pillar extracted at a time. These two approaches broadly approximate the "Christmas Tree" and "Outside Lift" methods, respectively. In both cases, the pillar removal proceeds from top-left (i1,j2) to bottom right (i5,j10) by first removing pillars in a given column (top to bottom) and then advancing to the adjacent column (left to right). In the first extraction method (two pillars at a time), the final pillar in each column was removed individually.

3. MODEL SETUP

NIOSH visited 30 retreat coal mines, located in Utah, Colorado, West Virginia, Virginia, and Kentucky and a majority of these mines were found to be operating at a depth between 300 m to 500 m (NIOSH, 2010). Accordingly, the adopted a coal mine layout has a seam thickness of 3 m with 6 m drifts (Zipf, 2001) at a depth of 400 m below the surface. The model extends up to 200 m below the surface and 75 m below the mining seam. The in situ vertical stress at the top of the coal seam (400 m) is 8.83 MPa. The k ratio was assumed to be 1 in the study.

As previously mentioned, two W/H ratios were modeled: 3 and 6. The resulting pillar dimensions for W/H=3 and W/H=6, in plan view, are 9 m x 9 m and 18 m x 18 m, respectively. The width and length extents of the model are dependent on the pillar W/H ratios. As the ratio increases, the mining panel area also increases. In addition, a 50 m abutment surrounding the pillar panel was added to the model.

3.1. Mesh Size

The mesh size varies throughout the model. Esterhuizen et al. (2010) states that a mesh size of 0.3 m to 0.33 m is typically satisfactory in modeling coal pillars. Accordingly, a mesh size of 0.33 m was used in the depth range 399 m to 404 m (1 m on either side of the coal seam). The mesh size was doubled to 0.66 m for the abutment area. The mesh size was increased to 1.3 m, 4 m, 8 m, and 12 m for regions further away from the coal seam. Figures 4 and 5 show how the mesh size varies throughout the model.

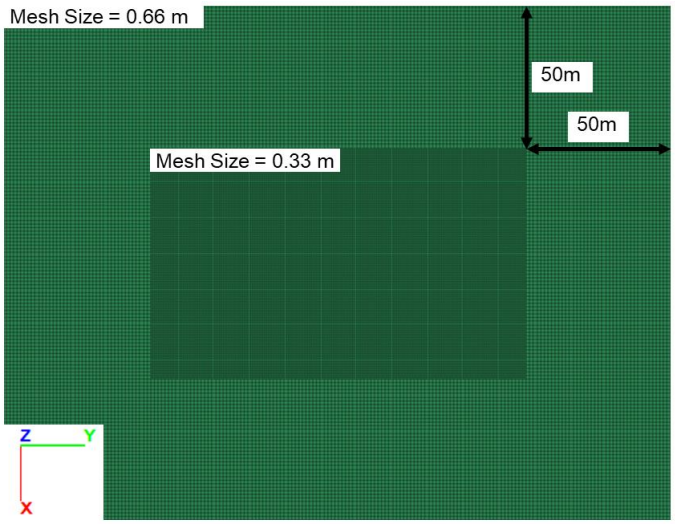

Fig. 4. Assigned mesh sizes from depth 399 m to 404 m.

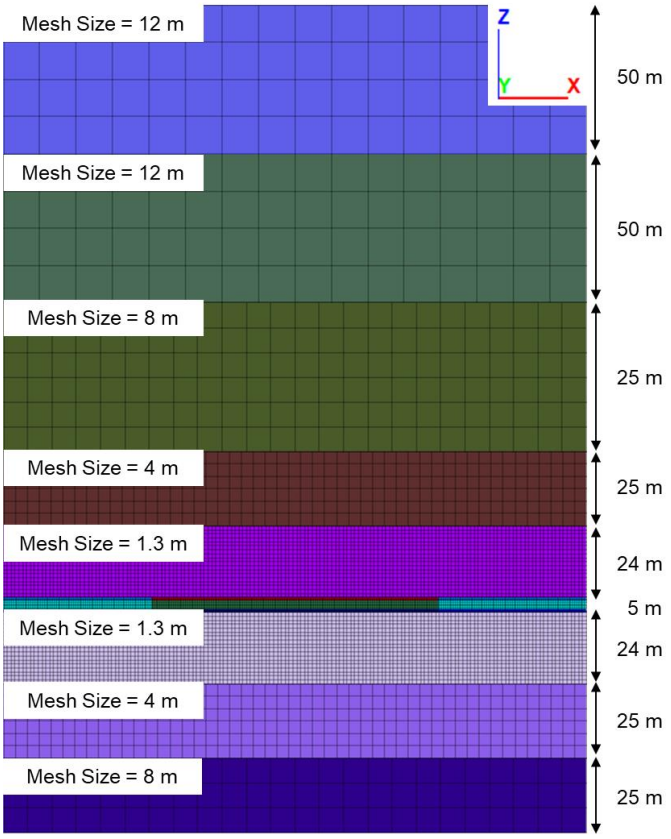

Fig. 5. Assigned mesh sizes to the model outside of 399 m and 404 m.

3.2. Input Parameters

A sensitivity analysis was performed in this study. Specifically, four parameters were considered: retreat method (one or two pillars extracted at a time), W/H pillar ratio, Young's Modulus of the overburden, and pillar material properties.

Two overburden Young's Modulus values were considered due to the variable ranges of Young's Modulus reported in the literature (Kumar et al., 2018). Ultimately, end-member values of 10 GPa (stiff roof) and 1 GPa (soft roof) were considered in this study.

Two sets of pillar material properties were considered: elastic and strain-softening. The results of the strain-softening cases were then compared to the corresponding elastic model results. In the strain-softening case, only the coal seam was modeled as inelastic; the surrounding material was modeled as elastic. The elastic properties used in the models are displayed in Table 1 (Kumar et al., 2018).

Table 1. Base model parameters and elastic properties

Material	Young's Modulus (GPa)	Density (kg/m^3)	Poisson's Ratio
Ore	3	1400	0.25
Host Rock	1 or 10	2250	0.25

Strain-softening parameters for the pillars were based on those from Esterhuizen et al. (2010), (see Table 2), who calibrated parameters to match an empirical pillar strength equation (Mark, 2000):

$$S_p = S_1(0.64 + 0.36\frac{w}{h}) \qquad (1)$$

One deviation from the parameters of Esterhuizen et al. (2010) is that the UCS value was reduced from 20 MPa to 16 MPa in order to model weaker properties; this was done to promote more pillar yield to simulate an upper bound in terms of difference from the elastic models. Additionally, the residual parameters shown in Table 2 were also reduced from those suggested by Esterhuizen et al. (2010). Specifically, the residual m and s parameters were reduced by 75%. The critical plastic shear strain was also reduced (to 0.02) and is half of the value that corresponds to that suggested by Esterhuizen et al. (2010), after accounting for the mesh size dependency of this parameter.

Using a lower critical plastic shear strain results in a greater rate of strength degradation, and simulates more brittle material. A higher critical shear strain 0.06 was also tested in a limited number of cases to highlight the sensitivity of the model results to this parameter. σ_3^{cv} (a parameter that demarcates the confinement above which a constant-volume flow rule is followed) was assigned a value of 0. With σ_3^{cv} set to 0, the dilation angle is effectively 0° (Itasca, 2016). Esterhuizen et al. (2010) found that non-zero values for σ_3^{cv} caused large

Table 2. Strain-softening parameters applied to the ore seam for the inelastic cases.

Parameter	Value
UCS (MPa)	16
m-value	1.47
s-value	0.07
a-value	0.65
m-residual	0.25
s-residual	0.00025
Plastic Shear strain	0.02
σ_3^{cv} (MPa)	0

Table 3. Naming convention for the models in this study.

Parameters	Elastic	Inelastic
W/H = 3 ; Soft Roof	Case 3E Soft	Case 3I Soft
W/H = 3 ; Stiff Roof	Case 3E Stiff	Case 3I Stiff
W/H = 6 ; Soft Roof	Case 6E Soft	Case 6I Soft
W/H = 6 ; Stiff Roof	Case 6E Stiff	Case 6I Stiff

distortions of the yielding elements which were deemed excessive.

The eight cases examined to determine the influence of inelastic pillar material behavior on the stress concentration trends predicted through the elastic approach are summarized in Table 3.

4. RESULTS

The results of this study focus on the differences in average pillar stresses between the inelastic (strain-softening) and elastic model cases. Results are shown as percentage difference relative to the elastic model. Positive percentage differences indicate that the stresses in the strain-softening model are less than those in the corresponding elastic model.

Before comparing the inelastic and elastic model cases, two strain-softening models with different critical plastic shear strain values (0.02 and 0.06) were compared. Case 3I Stiff and individual pillar extraction was considered. In this case, negative percentage difference values correspond to higher average stresses in the 0.06 case.

4.1. Influence of Critical Plastic Shear Strain

The results of the initial sensitivity analysis considering different values of the critical plastic shear strain shows that the pillar stress re-distribution process is notably influenced by the brittleness of the pillars. Figure 6 shows the percent difference between the stresses as a result of the critical plastic shear strain.

The development load condition is not shown in Figure 6, due to minimal differences in predicted stresses (< 0.5% average pillar stress). Once the retreat operations begin, the critical plastic shear strain impacts the behavior of the ore seam. The percent difference jumps from less than 0.5% (development load condition) to over 400% in some pillars. The large discrepancy is due to the fact that the critical plastic shear strain influences the degradation of the pillars. The negative values are associated with greater stresses in the 0.06 critical plastic shear strain case. These pillars experience less yielding and are able to continue to take on more load. In the case of the critical shear strain of 0.02, the pillars carry less stress as there is greater yielding in the pillars, causing them to shed stresses to the abutments.

4.2. Comparison of Inelastic and Elastic Models

The comparison of the inelastic and elastic models was performed for W/H ratios of 3 and 6. For each W/H ratio, pillars were removed either one at a time or two at a time under either a stiff or a soft roof. The models were compared by determining the % average stress difference. The % average stress difference was calculated using the average vertical stress through the pillar, in the inelastic material model and its corresponding elastic material model. A positive % average stress difference reflects greater predicted average vertical stress in the pillar under elastic conditions.

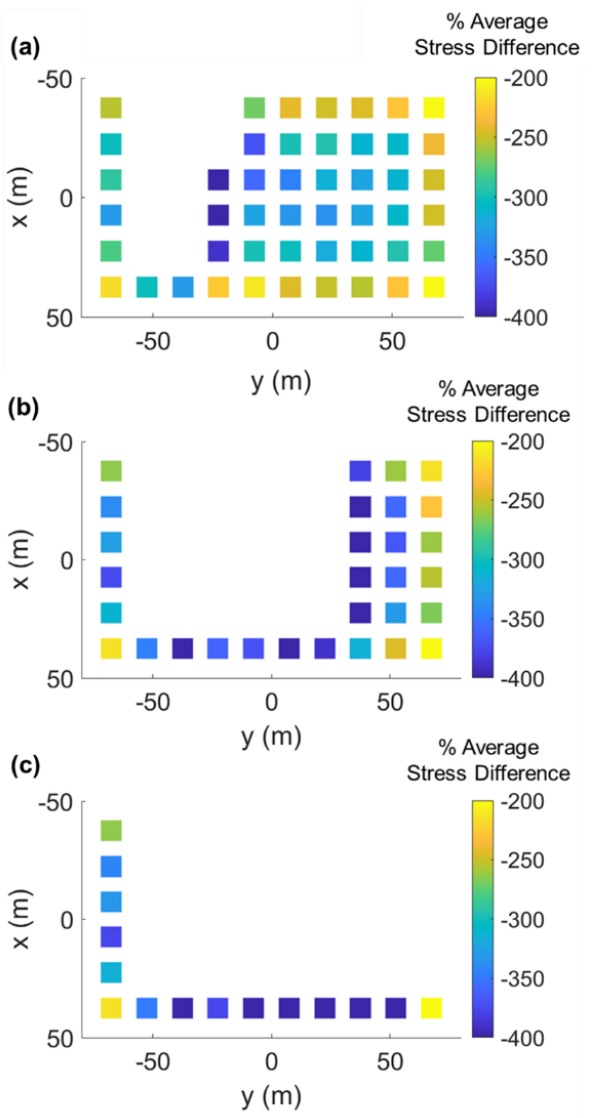

Fig. 6. Stress comparison between a critical plastic shear strain of 0.06 and 0.02. (a) Percent difference for pillar removal at stage i2j4. (b) Percent difference for pillar removal at stage i5j7. (c) Percent difference after all pillars are removed from the panel.

4.2.1. W/H of 3

In the W/H = 3 case, upon examining the average stress difference as a result of the sequencing of the pillar removal (one at a time versus two at a time), it was found that there was minimal impact on the model results. Because of this, more detailed results focused on the influence of pillar removal sequence are not presented. All results shown correspond to the case where one pillar was removed at a time.

Figure 7 represents the percent difference between Case 3I Stiff and Case 3E Stiff. Figure 8 shows the same results for Case 3I Soft and Case 3E Soft.

In both the stiff and soft roof models, the development load conditions (initial room and pillar) is relatively insensitive to the use of an inelastic constitutive model; this is because the initial development loading condition doesn't induce high enough stresses to generate significant yield in the pillars.

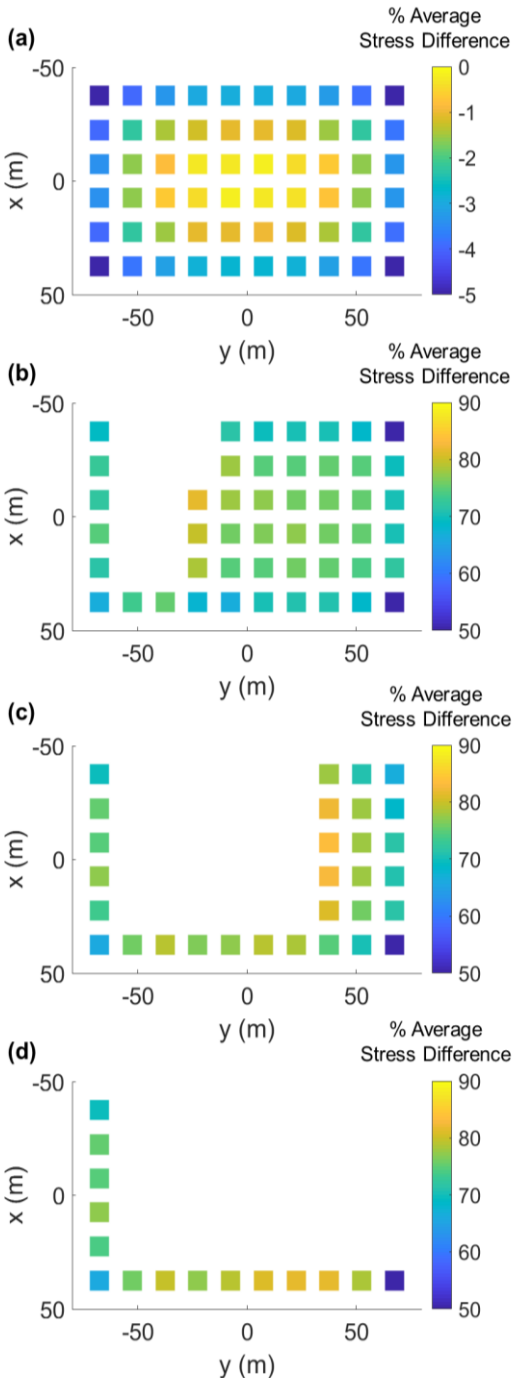

Fig. 7. Stress comparison between Case 3I Stiff and Case 3E Stiff: (a) Stress percent difference prior to pillar removal. (b) Percent difference for pillar removal at stage i2j4. (c) Percent difference for pillar removal at stage i5j7. (d) Percent difference after all pillars are removed from the panel. Note that the colorbar is different in Figure 6 (a). This is due to the small range reflected in the figure that does not lie within the range of (b), (c), or (d).

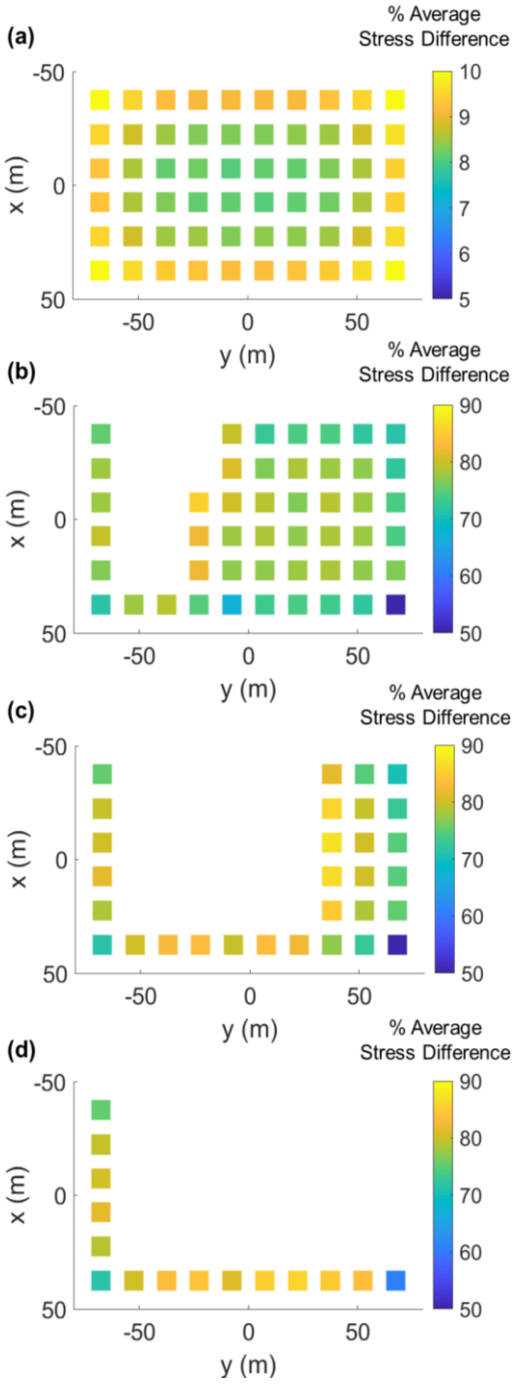

Fig. 8. Stress comparison between Case 3I Soft and Case 3E Soft: (a) Stress percent difference prior to pillar removal. (b) Percent difference for pillar removal at stage i2j4. (c) Percent difference for pillar removal at stage i5j7. (d) Percent difference after all pillars are removed from the panel. Note that the colorbar is different in Figure 6 (a). This is due to the small range reflected in the figure that does not lie within the range of (b), (c), or (d).

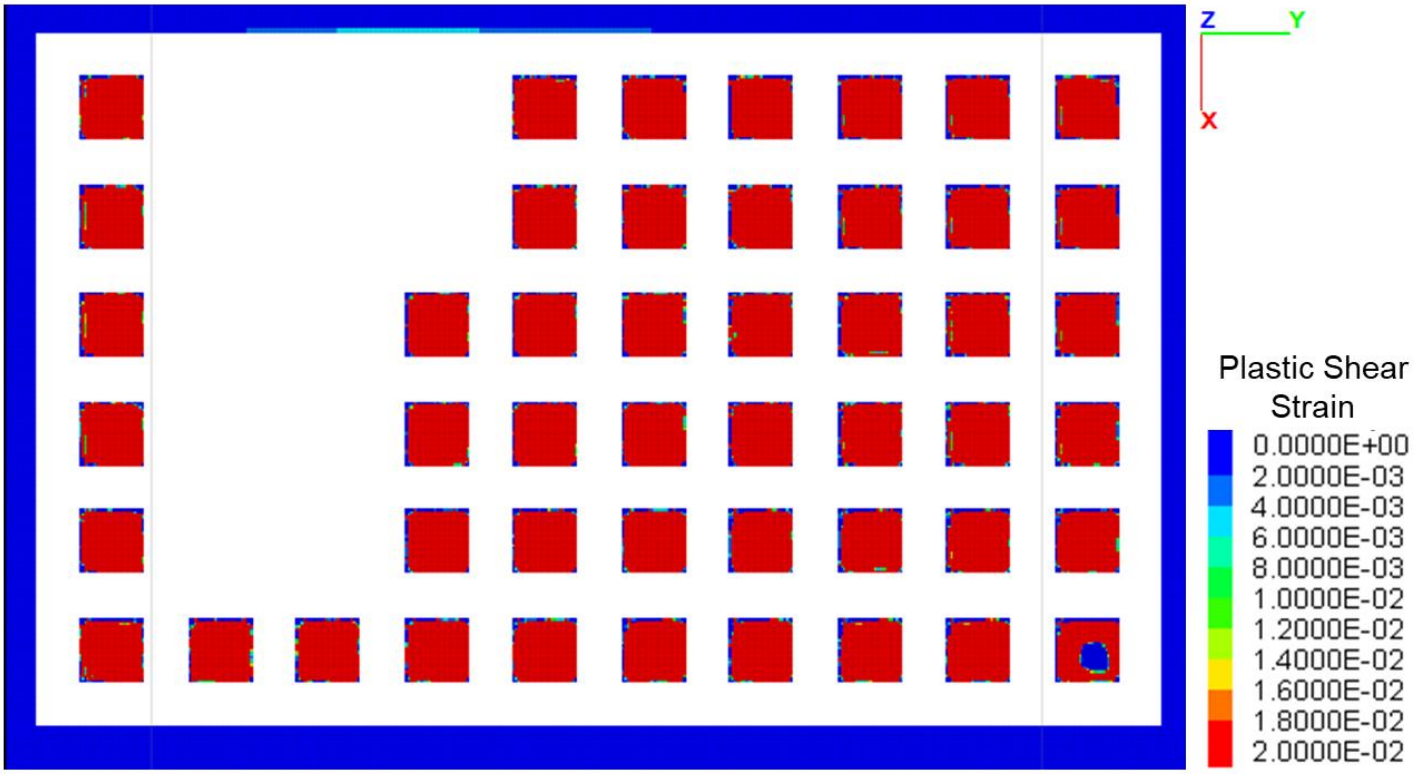

Fig. 9. Plastic shear strain within each pillar at the i2j4 retreat extraction stage for Case 3I Soft.

During the retreat process, stresses in Case 3I Stiff and Soft differ upwards of 80% from those in Case 3E Stiff and Soft. The stress difference is due to the yielding of the pillars adjacent to the excavated area in the inelastic model. As pillars are removed, the adjacent pillars take on more load. As the load on the pillars increases, the pillars experience more yield. The pillars continue to yield until they have reached their residual state and have shed most of their load. As a result, the pillars closest to the excavated area have the greatest % average stress difference. The % average stress difference then reduces moving towards the outer boundary, where pillars experience less stress difference.

Comparing the results of the stiff versus soft roof case, it is apparent that load yield extends further away from the excavated area in the soft roof case. This is supported by Mark's (2000) finding that stiffer roofs lead to less stress shedding and can therefore support smaller pillars.

Examining the model in FLAC^{3D} confirms the observation and the yielding of pillars with a W/H=3. At the i2j4 retreat extraction stage, almost all the pillars have yielded through their cores. The plastic shear strain values within the pillars are shown in Figure 9. A plastic shear strain value greater than 2E-2 indicates that the material is in its residual state. Such large extents of yielding can be a sign of improper mine (pillar) design and might lead to global failure during the retreat mining process.

4.2.2. W/H of 6

Like the W/H = 3 case, the W/H = 6 case also was minimally impacted by the pillar removal sequence. Thus, the results shown correspond to the cases where one pillar was removed at a time.
Figure 10 represents the percent difference between Case 6I Stiff and Case 6E Stiff. Figure 11 shows the same results for Case 6I Soft and Case 6E Soft.

Similarly, to the W/H = 3 cases, the development load stress conditions (initial room and pillar) are relatively insensitive to the use of an inelastic constitutive model.

During the retreat process, stresses in Case 6I Stiff and Soft differ upwards of 15% from those in Case 6E Stiff and Soft. The stress difference is due to the partial yielding of the pillars adjacent to the excavated area in the inelastic model. As pillars are removed, the adjacent pillars take on more load, resulting in yielding at the pillar edges. The pillars don't fully yield, and as a result load shedding onto surrounding pillars is minimal.

As in the W/H = 3 cases, the soft roof case results in stresses being shed further away from the yielding pillars near the excavated area.

Examining the model in FLAC^{3D} confirms the limited nature of the yielding of the W/H=6 pillars. It can be seen that at the i2j4 retreat extraction stage, yielding in the pillars occurs along the outer edges of the pillars adjacent to the extracted area. The plastic shear strain values within the pillars are shown in Figure 12. The yield

limited to pillars nearest to the excavated area, and only the edges of the pillars have yielded.

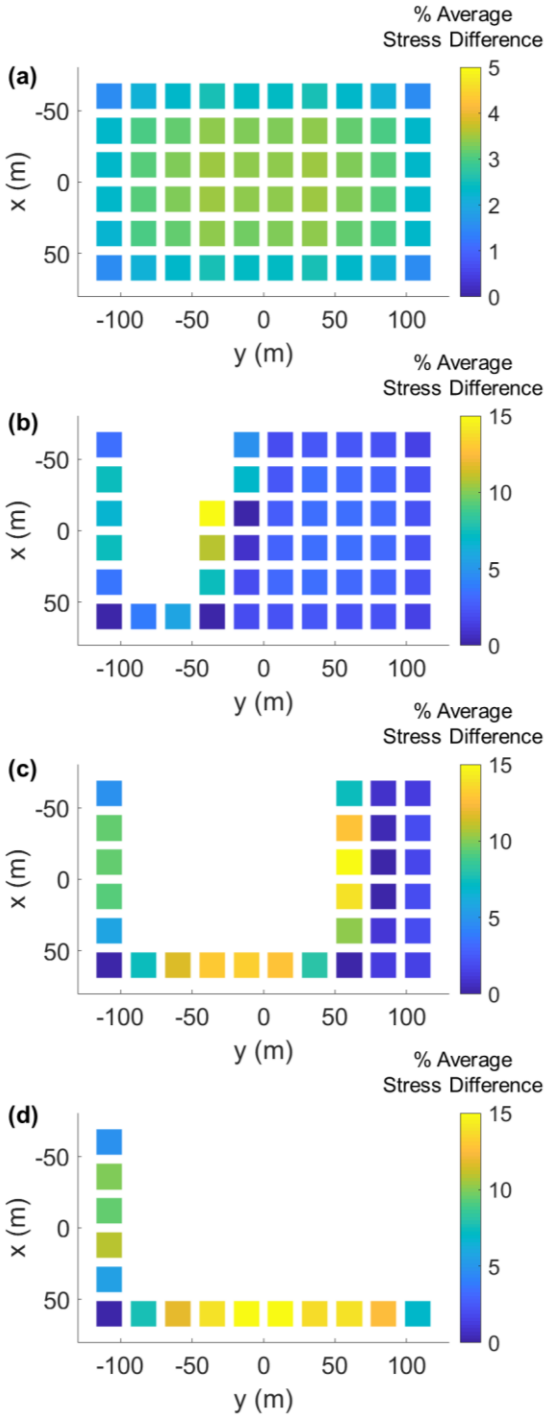

Fig. 10. Stress comparison between Case 6I Stiff and Case 6E Stiff: (a) Stress percent difference prior to pillar removal. (b) Percent difference for pillar removal at stage i2j4. (c) Percent difference for pillar removal at stage i5j7. (d) Percent difference after all pillars are removed from the panel. Note that the colorbar is different in Figure 6 (a). This is due to the small range reflected in the figure that does not lie within the range of (b), (c), or (d).

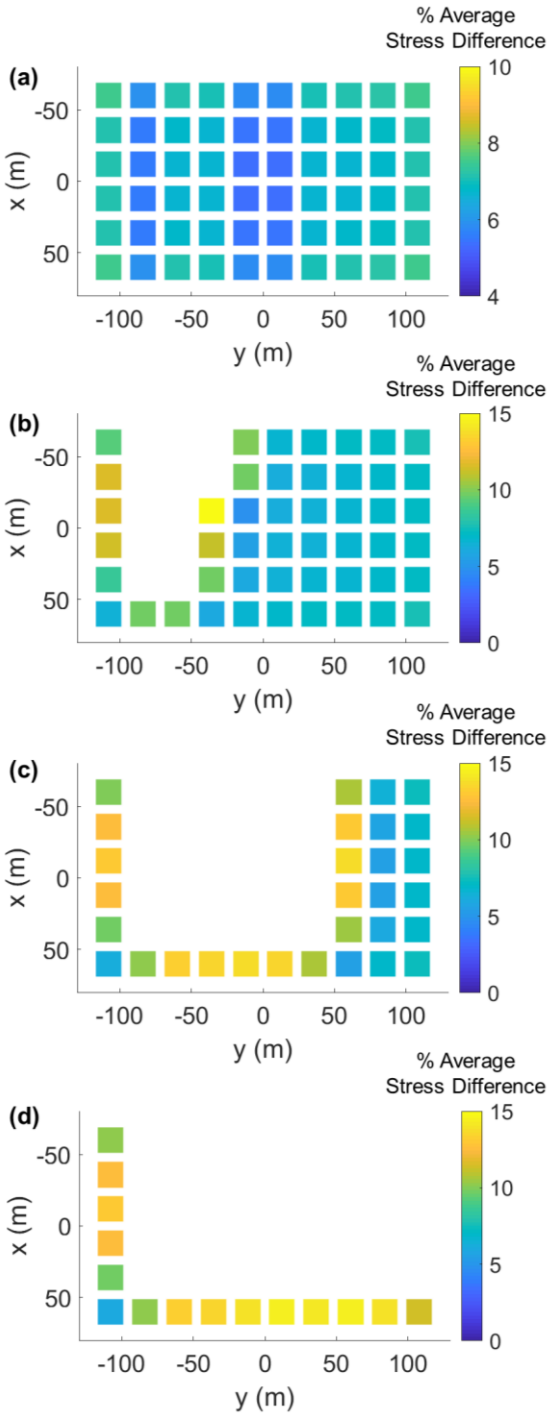

Fig. 11. Stress comparison between Case 6I Soft and Case 6E Soft: (a) Stress percent difference prior to pillar removal. (b) Percent difference for pillar removal at stage i2j4. (c) Percent difference for pillar removal at stage i5j7. (d) Percent difference after all pillars are removed from the panel. Note that the colorbar is different in Figure 6 (a). This is due to the small range reflected in the figure that does not lie within the range of (b), (c), or (d).

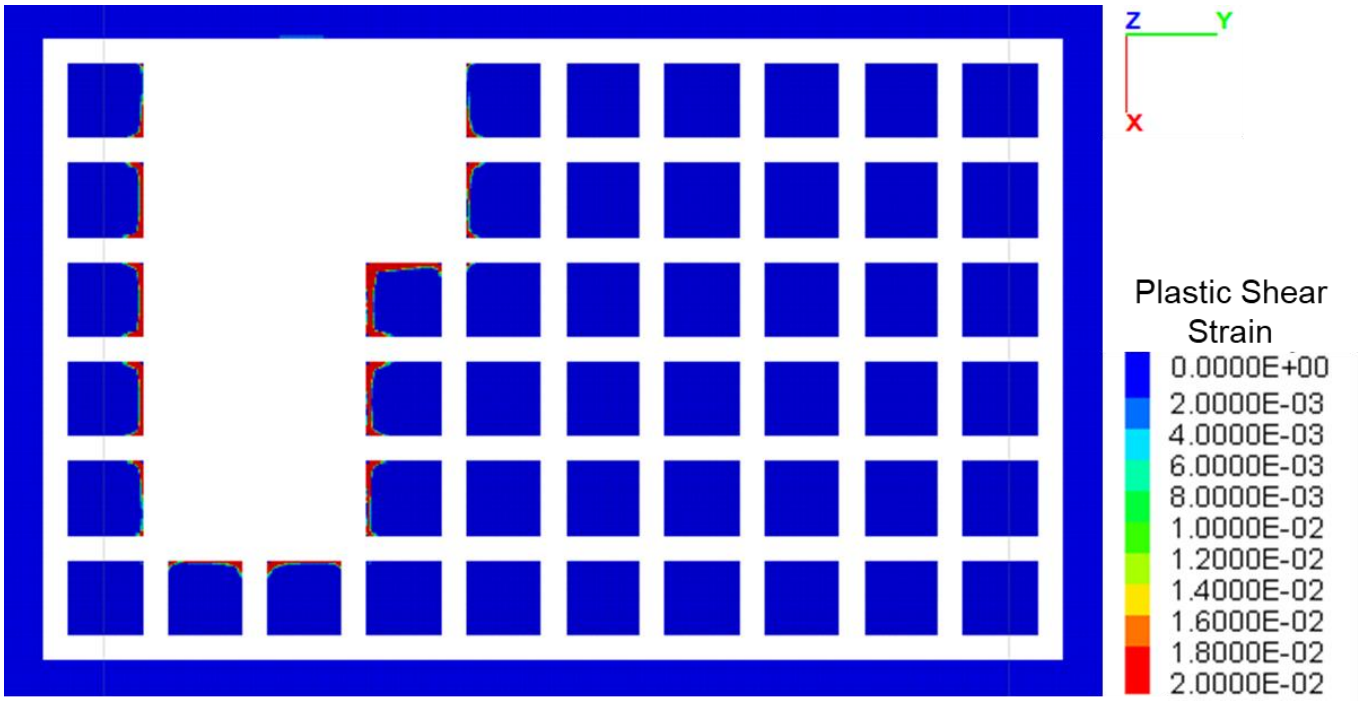

Fig. 12. Plastic shear strain within each pillar at the i2j4 retreat extraction stage for Case 6I Soft.

5. DISCUSSION

From the results of the various models that were run as a part of this study, it can be seen that modeling with elastic properties may result in incorrect pillar stress estimations. Prior to removal of any pillars, there is minimal % average stress difference between the inelastic and elastic model. Thus, the impact of modeling the development stage as elastic or inelastic is insignificant (although this will be specific to the geomining conditions considered). However, as the retreat process commences, the differences between the inelastic and elastic models become significant. As pillars are removed, the elastic models begin to incorrectly estimate the pillar stresses. This is because stresses start shedding to surrounding pillars. The observation correlates with Frith and Reed's (2017) observations that elastic model results are conservative. The inelastic models have the potential to provide a more realistic representation of stresses in the pillars.

Besides the elastic versus inelastic difference, the greatest influence appears to be a result of the W/H pillar ratio. In the case of a W/H = 3, the stresses differed in excess of 75%, whereas, for a W/H = 6 the stresses rarely differed between the elastic and inelastic cases by more than 15%. The primary reason is that pillar yield is impacted by the W/H ratio of the pillar (see Figure 7 through 11). This is largely because the W/H ratio influences the extraction ratio, which in turn influences the resulting stresses. Considering the W/H ratio as part of the TAT equation (Eq.2), it can be observed how greater W/H ratios pillars are expected to have greater stresses (Pariseau, 2007).

$$Stress = \gamma * D \left(\frac{w+h}{w}\right)^2 \qquad (2)$$

γ is the unit weight of the rock, D is the depth, w is the pillar width, and h is the drift width. Inputting the model geometry parameters used in the W/H of 3 and 6 models, the estimated stresses as a function of γ * D are as follows:

- W/H of 3 = $\left(\frac{9+6}{3}\right)^2$* γ *D
- W/H of 6 = $\left(\frac{18+6}{3}\right)^2$* γ *D

TAT shows that increasing the W/H ratio (while keeping entry width constant) results in an increase in stress within the pillar. The lower stress combined with the geometric strengthening effects associated with higher W/H pillar ratios leads to less yield throughout the retreat mining operation.

The yielding of the pillars significantly impacts the stress redistribution throughout the retreat process. Yielding of the pillars begins along the edges and then propagates towards the center of the pillar. With continued loading, the pillar attains its residual strength and is unable to take on additional load. This causes the surrounding pillars to take on that load, thereby causing these pillars to yield.

In the models, it was found that the stiff roof cases result in less load transfer than the soft roof case. In the soft roof case, load transfers further away from the excavated area. This is because stiff roofs will flex less than soft roofs. This results in soft roofs being able to deflect and transfer loads over greater distances.

6. CONCLUSIONS

The study shows that in retreat mining applications, the stress redistribution process is highly sensitive to the geometric and material parameters that control pillar yield. The excavation ratio, as influenced by the W/H pillar ratio in this case, influences the resulting pillar stresses and yield. Stress will redistribute beyond the excavated area as pillars yield and shed load to surrounding pillars. This was found to be extreme in the W/H cases with a higher extraction ratio.

In addition, the influence of stiff and soft roofs is notable when examining the extent loads are redistributed. Soft roofs (low Young's Modulus) are shown to result in greater load transfer away from the excavated area than stiff roofs (high Young's Modulus). The distance the load distributes away from the excavated area is a result of the corresponding flexural rigidity of the roof. In the study, the greater distances loads are able to distribute, the more yield a pillar was subjected to and the % average stress difference between inelastic and elastic models was correspondingly larger.

Predictions of pillar stresses made using elastic models may not be sufficient in some cases. The elastic model is conservative in that it provides a maximum stress prediction that can be used for comparison with pillar strength as estimated outside the model. The inelastic models consider the dynamic interaction between stress and strength as pillars yield during retreat mining operations.

ACKNOWLEDGEMENTS

The research conducted for this study was also partially funded by the National Institute of Occupational Health and Science (NIOSH) under Grant Number 200-2016-90154.

Part of the modeling effort for this study was conducted as part of a graduate course entitled "Applied Numerical Modeling for Geomechanics" using educational licenses of FLAC^{3D} provided by Itasca Consulting, Ltd. The authors appreciate Itasca's support in this capacity.

In addition, the authors appreciate the efforts of Sankhaneel Sinha for providing review and feedback on the paper.

REFERENCES

1. Esterhuizen, E., C Mark, and M. M. Murphy. 2010. Numerical model calibration for simulating coal pillars, gob and overburden response. In *Proceeding of the 29th international conference on ground control in mining, Morgantown, WV* (pp. 46-57).
2. Frith, R., & G Reed. (2017). Coal Pillar Design When Considered As An Overburden Reinforcement Rather Than Suspension Problem. In *Proceedings of the 36th International Conference on Ground Control in Mining* (pp. 1-11).
3. Itasca. (2016) FLAC 3D Hoek-Brown_PAC Model Versionv6. Itasca Consulting Group, Minneapolis, Minnesota
4. Kumar A., R Singh., and P Waclawik. 2018. Numerical Modelling Based Investigation of Coal Pillar Stability for Room and Pillar Development at 900 m Depth of Cover. *Proceedings of the 37th International Conference on Ground Control in Mining*
5. Mark, C. 2. (2000). State-of-the-art in coal pillar design. *Transactions-Society for Mining Metallurgy and Exploration Incorporated*, *308*, 123-128.
6. Mark, C. 2009. Deep cover pillar recovery in the US. In *Proceedings of the 28th International Conference on Ground Control in Mining* (pp. 1-9).
7. NIOSH. 2010. Research Report on the Coal Pillar Recovery under Deep Cover. Retrieved from https://www.cdc.gov/niosh/mining/UserFiles/works/pdfs/Report_on_Coal_Pillar_Recovery_under_Deep_Cover_02-10.pdf.
8. Pariseau, W.G., 2007, Design Analysis in Rock Mechanics, Taylor & Francis, Great Britain, 278-289.
9. Ünlü, T. (2001). Critical dimension concept in pillar stability. In *Proceedings of the 17th international mining congress and exhibition of Turkey* (pp. 341-347).
10. Zipf, R. K. 2001. Toward Pillar Design to Prevent Collapse of Room-and-Pillar Mines. 2011. In *108th Annual Exhibit and Meeting, Society for Mining, Metallurgy, and Exploration, Denver, CO, 26-28 February*.